

# Monte Carlo Localization Using the Filter-Based Random Motion Model in Wireless Sensor Networks

<sup>1</sup>Jung Min Pak, <sup>\*2</sup>Dong Won Kim

<sup>1</sup>Department of Electrical Engineering,

Wonkwang University, Iksan, Jeonbuk, South Korea, E-mail: destin11@wku.ac.kr

<sup>\*2</sup>Department of Digital Electronics,

Inha Technical College, Incheon, South Korea, E-mail: dwnkim@inhac.ac.kr

## Abstract

*This paper proposes a new motion model for the Monte Carlo localization in wireless sensor networks. The existing constant velocity motion model (CVMM) exhibits poor localization performance if the process noise is inappropriately modeled. To overcome this problem, we propose the filter-based random motion model (FBRMM) as an alternative to the CVMM. The FBRMM uses pseudo control commands, which are modeled as Gaussian random variables based on the information obtained from the filter. The FBRMM does not require the process noise modeling and provides better localization performance compared with the CVMM.*

**Keywords:** Indoor localization, filter-based random motion model (FBRMM), Monte Carlo localization, state estimation, wireless sensor network.

## 1. Introduction

Indoor real-time localization systems (RTLSS) based on wireless sensor networks (WSNs) [14-16] have attracted much attention of users in various industrial fields, such as construction sites, hospitals, and logistics [1-9]. The RTLSS based on WSN uses transmission of radio signal between the transmitter and the receiver, in which various types of measurements, such as the time of arrival (TOA), time difference of arrival (TDOA), and angle of arrival (AOA) can be used [1]. In indoor environment, wireless signals contain much noise and this can degrade the localization accuracy. Thus, stochastic filters (i.e., state estimators) are typically used to estimate the position of a target object from the noisy measurements [2], [3]. The most renowned stochastic filter is the Kalman filter (KF), which is an optimal estimator for linear systems with Gaussian noise. The extended KF (EKF) and the unscented KF (UKF) are nonlinear filters [10]. Measurements used in WSNs including the TOA, TDOA, and AOA are represented by nonlinear equations, and thus nonlinear filters are used for the localization based on WSNs.

Monte Carlo localization (MCL) refers to the localization using the particle filter (PF) [11]. Compared to the nonlinear KFs, the PF has several advantages when used for localization. First, the PF can perform the global localization, which is the situation of unknown initial position. Second, the PF exhibits better performance than the nonlinear KFs in nonlinear/non-Gaussian systems. Thus, we consider the MCL based on the PF for the RTLSS [10], [11].

When applying the MCL to the RTLSS, the motion model plays an important role; that is to obtain useful information on the motion of a target object. In the mobile robot localization, a target object (i.e., robot) can transmit useful information on its motion. Mobile robots usually equip with sensors to measure the bearing angle or the rotational speed of wheels. Thus, information on the bearing angle and speed of the robot can be obtained. This type of localization is called the active localization. On the contrary, if the target objects are human, equipment, and goods, the motion information is not available. This type of localization is called the passive

---

\* Corresponding Author

Received: Nov. 10, 2016, Revised: Feb. 4, 2017, Accepted: Mar. 27, 2017

localization. In cases of passive localization, the constant velocity motion model (CVMM) is typically used as a motion model [4–7].

The CVMM assumes that the velocity (speed and course) is constant for a short sampling time. This assumption fits to the situation where the sampling time is very short or the actual velocity is constant. If the change in the velocity is abrupt and significant, modeling error between the CVMM and the real motion occurs, which leads to the degradation of localization accuracy [4–7]. Another disadvantage of the CVMM is a burden of selecting the process noise covariance  $\mathbf{Q}_k$ . In the CVMM, the process noise reflects the amount of motion change. If  $\mathbf{Q}_k$  is too small or too large, the localization using the CVMM may exhibit poor performance [12]. However, selecting an appropriate value of  $\mathbf{Q}_k$  is difficult because  $\mathbf{Q}_k$  is intrinsically uncertain. Thus, selection of  $\mathbf{Q}_k$  is a burden for the designers of localization systems.

In this paper, we propose a new motion model to overcome the drawbacks of the conventional CVMM. The proposed motion model assumes that the motion is governed by pseudo control commands. The pseudo control commands are modeled as Gaussian random variables, and the mean and the covariance are calculated using the position information obtained from the stochastic filter. Thus, the proposed motion model is called the filter-based random motion model (FBRMM). Through simulations, we demonstrate that the proposed FBRMM exhibits better localization performance than the conventional CVMM in the MCL using the WSNs.

The rest of this paper is organized as follows. In Section 2, a typical MCL scheme is explained and a new motion model for the MCL, called the FBRMM, is proposed. In Section 3, MCL simulation results comparing the FBRMM with the existing CVMM are presented. Finally, the conclusion is given in Section 4.

## 2. Main Results

In this section, the MCL in wireless sensor networks is described. First, a typical MCL scheme is explained, and then, a new motion model called the FBRMM is proposed to improve the robustness of the MCL.

### 2.1. Monte Carlo Localization Scheme in Wireless Sensor Networks

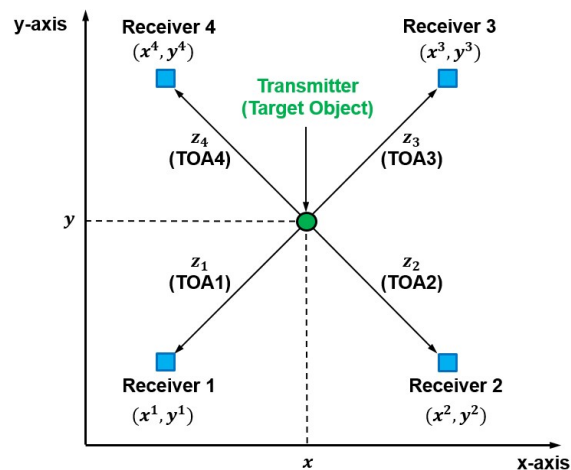


Fig. 1 2D schematic of wireless sensor network

We consider a WSN consisting of four receivers and a transmitter as shown in Fig. 1. The transmitter is attached to a target object, such as human, equipment, and goods. Radio signal transmits from the transmitter to the receivers, the signal transmission time, the TOA, is measured. Given the

four TOA measurements, position of the transmitter can be estimated by filters (i.e., state estimators), which requires a state-space model describing the motion and the measurements. The TOA measurements is modeled as follows.

$$z_{i,k} = \frac{1}{c} \sqrt{(x_{i,k} - x_k)^2 + (y_{i,k} - y_k)^2} \quad (i = 1, 2, 3, 4), \quad (1)$$

where  $z_{i,k}$  is the  $i$ -th TOA measurement at time  $k$ ,  $(x_{i,k}, y_{i,k})$  is the 2 dimensional (2D) position of the  $i$ -th receiver,  $(x_k, y_k)$  is the 2D position of the transmitter, and  $c$  is the speed of light. The measurement vector consisting of four TOA measurements is defined as  $\mathbf{z}_k = [z_{1,k} \ z_{2,k} \ z_{3,k} \ z_{4,k}]^T$ .

---

**Algorithm 1: MCL based on RPF**


---

```

1 begin
2   - Generate initial samples (particles) of the state estimate:  $\{\mathbf{x}_0^i\}_{i=1}^N$ 
3   for  $k = 1, 2, \dots$  do
4     for  $i = 1 : N$  do
5       -  $\mathbf{x}_k^i = \mathbf{f}_{k-1}(\mathbf{x}_{k-1}^i, \mathbf{w}_{k-1})$ 
6       -  $\tilde{w}_k^i = \frac{1}{\sqrt{(2\pi)^{n_x} \det(\mathbf{R}_k)}} \exp\left\{-\frac{1}{2}(\mathbf{z}_k - \mathbf{h}_k(\mathbf{x}_k^i))^T \mathbf{R}_k^{-1}(\mathbf{z}_k - \mathbf{h}_k(\mathbf{x}_k^i))\right\}$ 
7     end for
8     - Calculate total weight:  $t = \sum_{i=1}^N \tilde{w}_k^i$ 
9     for  $i = 1 : N$  do
10      - Normalize the weight:  $w_k^i = t^{-1} \tilde{w}_k^i$ 
11    end for
12    - Calculate the empirical covariance matrix  $\mathbf{S}_k$  of the sample set  $\{\mathbf{x}_k^i\}_{i=1}^N$ .
13    - Compute  $\mathbf{D}_k$  such that  $\mathbf{D}_k \mathbf{D}_k^T = \mathbf{S}_k$ .
14    - Initialize the cumulative sum of weights (CSW):  $c_1 = w_k^1$ 
15    for  $i = 2 : N$  do
16      -  $c_i = c_{i-1} + w_k^i$ 
17    end for
18    -  $u_1 \sim \mathcal{U}[0, N-1]$ 
19    for  $j = 1 : N$  do
20      -  $u_j = u_1 + N^{-1}(j-1)$ 
21      while  $u_j > c_i$  do
22        -  $i = i + 1$ 
23      end while
24      -  $\mathbf{x}_k^{j*} = \mathbf{x}_k^i$ 
25    end for
26    for  $i = 1 : N$  do
27      - Draw  $\epsilon^i \sim K$ 
28      -  $\mathbf{x}_k^{i**} = \mathbf{x}_k^{i*} + h_{opt} \mathbf{D}_k \epsilon^i$ 
29    end for
30    -  $\hat{\mathbf{x}}_k = N^{-1} \sum_{i=1}^N \mathbf{x}_k^{i**}$ 
31  end for
32 end

```

---

Passive localization systems typically adopt the CVMM as a motion model. The CVMM for the 2D localization is described as

$$\begin{bmatrix} x_{k+1} \\ y_{k+1} \\ \dot{x}_{k+1} \\ \dot{y}_{k+1} \end{bmatrix} = \begin{bmatrix} 1 & 0 & T & 0 \\ 0 & 1 & 0 & T \\ 0 & 0 & 1 & 0 \\ 0 & 0 & 0 & 1 \end{bmatrix} \begin{bmatrix} x_k \\ y_k \\ \dot{x}_k \\ \dot{y}_k \end{bmatrix} + \begin{bmatrix} T^2/2 & 0 \\ 0 & T^2/2 \\ T & 0 \\ 0 & T \end{bmatrix} \mathbf{w}_k, \quad (2)$$

where  $(\dot{x}_k, \dot{y}_k)$  is the 2D velocity,  $T$  is the sampling interval, and  $\mathbf{w}_k \in \mathbb{R}^2$  is the process noise vector. We assume that  $\mathbf{w}_k$  is a zero-mean white Gaussian noise vector with the covariance matrix  $\mathbf{Q}_k$ . From (2), the state vector is defined as  $\mathbf{x}_k = [x_k \ \dot{x}_k \ y_k \ \dot{y}_k]^T$ . Using this definition, the measurement model consisting of four TOA measurements is represented as

$$\mathbf{z}_k = \mathbf{h}_k(\mathbf{x}_k) + \mathbf{v}_k, \quad (3)$$

where  $\mathbf{h}_k = [h_{1,k} \ h_{2,k} \ h_{3,k} \ h_{4,k}]^T$  is the nonlinear operator that computes the four TOA measurements based on (1). In addition,  $\mathbf{v}_k \in \mathbb{R}^4$  is the measurement noise vector, which is assumed to be zero-mean white Gaussian and its covariance is  $\mathbf{R}_k$ .

The MCL is conducted by applying the PF to the state-space model that consists of the motion model (2) and the measurement model (3). Although there are various versions of PFs, we use the regularized PF (RPF) [13] because it is robust against sample impoverishment and is easy to implement. The algorithm of the MCL based on the RPF can be described by **Algorithm 1**. For the RPF, we use the Gaussian kernel. The optimal bandwidth for the Gaussian kernel,  $h_{opt}$ , can be computed as

$$h_{opt} = [4 / (n_x + 2)]^{1/n_x+4} N^{-1/n_x+4}, \quad (4)$$

where  $n_x$  is the state vector dimension, and  $N$  is the number of particles.

## 2.2. Filter-Based Random Motion Model

As described in Section 1, the CVMM has several disadvantages. Thus, we propose a new motion model called the FBRMM for the MCL in WSNs. In the FBRMM, the state vector consists of three components: the 2D coordinate  $(x, y)$  and the heading (bearing) angle  $\theta$ . Then, the state vector at time index  $k$  can be defined as  $\mathbf{x}_k = [x_k \ y_k \ \theta_k]^T$ . We consider the control input vector,  $\mathbf{u}_k = [\Delta d_k \ \Delta \theta_k]^T$ , where  $\Delta d_k$  is the incremental distance and  $\Delta \theta_k$  is the incremental change in heading angle. Using these definitions of the state and control vectors, incremental changes in the 2D position can be described as follows:

$$x_{k+1} = x_k + \Delta d_k \cos\left(\theta_{k-1} + \frac{1}{2}\Delta\theta_k\right), \quad (4)$$

$$y_{k+1} = y_k + \Delta d_k \sin\left(\theta_{k-1} + \frac{1}{2}\Delta\theta_k\right), \quad (5)$$

$$\theta_{k+1} = \theta_k + \Delta\theta_k. \quad (6)$$

Considering the process noise, the motion model can be represented in a vector form as

$$\mathbf{x}_{k+1} = \mathbf{f}_k(\mathbf{x}_k) + \mathbf{w}_k, \quad (7)$$

where  $\mathbf{w}_k \in \mathbb{R}^3$  is the process noise, and  $\mathbf{f}_k = [f_{1,k} \ f_{2,k} \ f_{3,k}]^T$  is the nonlinear function that computes  $\mathbf{x}_{k+1}$  from the  $\mathbf{x}_k$  as defined in (4)–(6). This motion model has been used for the robot localization, in which the control command  $\mathbf{u}_k$  is available. This ‘robot motion model’ results in better accuracy than the CVMM because of the motion information in  $\mathbf{u}_k$ . However, the robot motion model is not applicable to the passive localization, because  $\mathbf{u}_k$  is not available. In this paper, we propose a novel method, the FBRMM, to use the robot motion model for the passive localization.

In the proposed FBRMM, the control commands  $u_{1,k} \triangleq \Delta d_k$  and  $u_{2,k} \triangleq \Delta \theta_k$  are modeled by Gaussian random variables as follows:

$$u_{1,k} \sim N(\mu_{1,k}, \sigma_{1,k}^2), \quad u_{2,k} \sim N(\mu_{2,k}, \sigma_{2,k}^2), \quad (8)$$

The mean and covariance values are calculated using the position data obtained from the filter as follows:

$$\mu_{1,k} = \frac{1}{n} \sum_{i=1}^n (d_i - d_{i-1}), \quad d_i = \sqrt{(\hat{x}_{k-i} - \hat{x}_{k-i-1})^2 + (\hat{y}_{k-i} - \hat{y}_{k-i-1})^2}, \quad (9)$$

$$\sigma_{1,k}^2 = \frac{1}{n+1} \sum_{i=1}^n (d_i - \mu_{1,k})^2, \quad (10)$$

$$\mu_{2,k} = \frac{1}{n} \sum_{i=1}^n (\phi_i - \phi_{i-1}), \quad \phi_i = \tan^{-1} \left( \frac{\hat{y}_{k-i} - \hat{y}_{k-i-1}}{\hat{x}_{k-i} - \hat{x}_{k-i-1}} \right), \quad (11)$$

$$\sigma_{2,k}^2 = \frac{1}{n+1} \sum_{i=1}^n (\phi_i - \mu_{2,k})^2, \quad (12)$$

where  $(\hat{x}_k, \hat{y}_k)$  is the 2D position estimated by a filter, and  $n$  is the averaging interval. In the FBRMM, the motion is governed by the control commands that are modeled by random variables as (9)–(12). By generating the random pseudo control commands  $u_{1,k}$  and  $u_{2,k}$  at each time step, we can use the FBRMM in the MCL.

### 3. Simulation

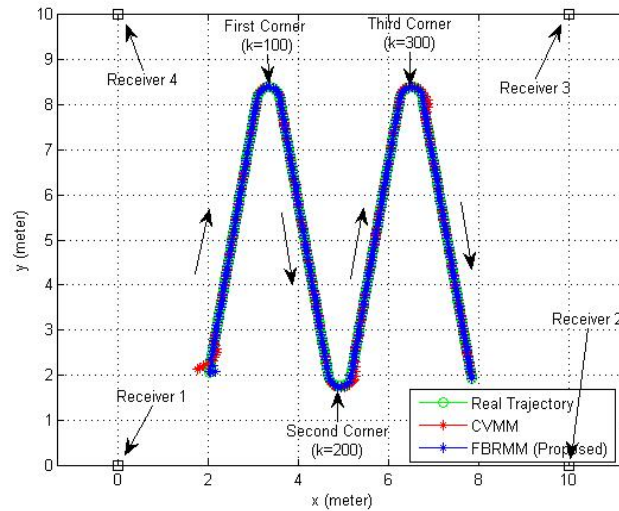
In this section, we test the proposed FBRMM through the MCL in a WSN. The simulation scenario is as follows. A person equipped with a transmitter moves in indoor environment. The indoor space is square shape, and its size is  $10\text{ m} \times 10\text{ m}$ . The person departs from the position (2, 2) and moves along a zigzag trajectory as shown in Fig. 2 (a). The four receivers are positioned at the corners, their coordinates are (0, 0), (10, 0), (10, 10), and (0, 10). The four TOA measurements are obtained and processed by the RPF (Algorithm 1). We consider two motion models: the existing CVMM and the proposed FBRMM. In the MCL based on the RPF, we compare the CVMM and the FBRMM. For the performance comparison, we use the localization error, which is defined as

$$E_k = \sqrt{(x_k - \hat{x}_k)^2 + (y_k - \hat{y}_k)^2}. \quad (13)$$

In the simulations, the averaging interval of the FBRMM is set as  $n=10$ . The measurement noise covariance is set as  $\mathbf{R}_k = 0.1^2 \mathbf{I}_4$ . In this paper, we use  $\mathbf{I}_m$  is the  $m \times m$  identity matrix. For the CVMM, we should set the process noise covariance  $\mathbf{Q}_k$ . However,  $\mathbf{Q}_k$  is very uncertain parameter. Thus, we set  $\mathbf{Q}_k = \mathbf{I}_2$  at the first, and then varies the value of  $\mathbf{Q}_k$ . Fig. 2 shows the results of MCL using the CVMM and the FBRMM. We see that the MCL using the CVMM exhibits rises in localization error near the second corner ( $k=200$ ) and the third corner ( $k=300$ ). This indicates that

$\mathbf{Q}_k$  is small compared to the changes in the real motion. The value of  $\mathbf{Q}_k$  is related to the amount of changes in real motion (speed and course). When the amount of motion change is large,  $\mathbf{Q}_k$  should be large. If  $\mathbf{Q}_k$  is small compared to the motion change, modeling error in the CVMM occurs, which leads to increase of estimation error. Due to a small  $\mathbf{Q}_k$  the estimation error of the CVMM rises around  $k = 200$  and  $k = 300$  where the course abruptly changes. In Fig. 2, the MCL using the FBRMM successfully works and does not exhibit sharp rise of estimation error around the corners.

In turn, we increased  $\mathbf{Q}_k$  to be  $10^2 \mathbf{I}_2$ . Fig. 3 shows the MCL results when  $\mathbf{Q}_k = 10^2 \mathbf{I}_2$ . Due to the increased  $\mathbf{Q}_k$ , the CVMM results in good localization results with very low estimation errors. This indicates  $\mathbf{Q}_k = 10^2 \mathbf{I}_2$  is a good choice. We further increased  $\mathbf{Q}_k$ . Fig. 4 shows the MCL results when  $\mathbf{Q}_k = 50^2 \mathbf{I}_2$ . In this figure, the MCL using the CVMM exhibits large estimation errors with oscillation. This is due to the large process noise. Too large value of  $\mathbf{Q}_k$  causes degradation of localization performance. Finally, we decreased  $\mathbf{Q}_k$  to be  $0.1^2 \mathbf{I}_2$ . Fig. 5 shows the simulation results when  $\mathbf{Q}_k = 0.1^2 \mathbf{I}_2$ . We see that the MCL using the CVMM diverges. In the MCL, a too small process/measurement noise causes sample impoverishment, which leads to localization failures. Fig. 5 shows the case of sample impoverishment due to a small  $\mathbf{Q}_k$ . In Figs. 2–5, we found that the performance of the CVMM depends on  $\mathbf{Q}_k$ . However,  $\mathbf{Q}_k$  is uncertain parameter and appropriate selection of  $\mathbf{Q}_k$  is difficult. On the contrary, the proposed FBRMM does not require selection of the process noise. Thus, users and designers are free from the difficult modeling of process noise.



(a)

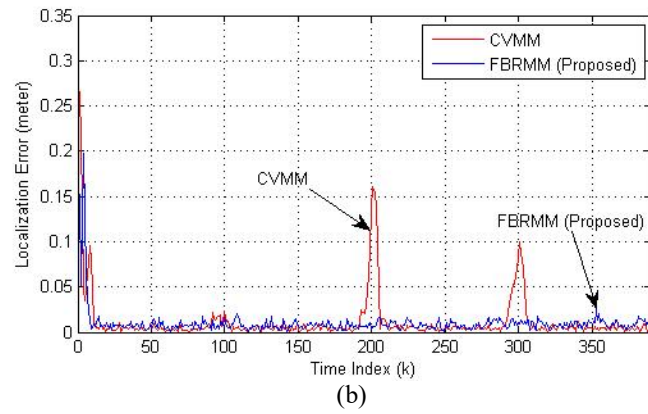


Fig. 2 MCL results when  $Q_k = I_2$ : (a) real and estimated trajectory and (b) localization error.

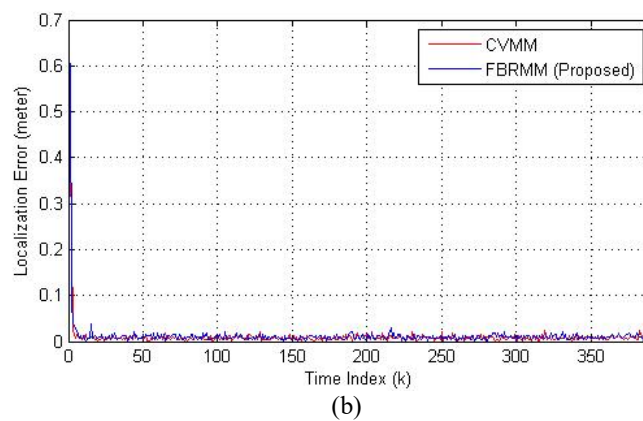
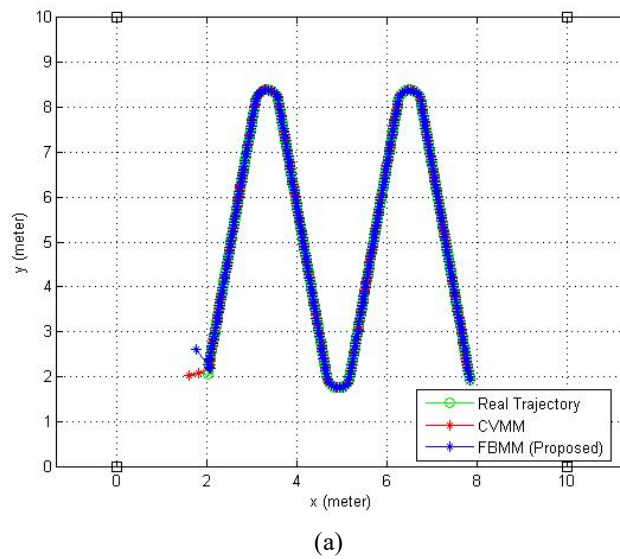


Fig. 3 MCL results when  $Q_k = 10^2 I_2$ : (a) real and estimated trajectory and (b) localization error.

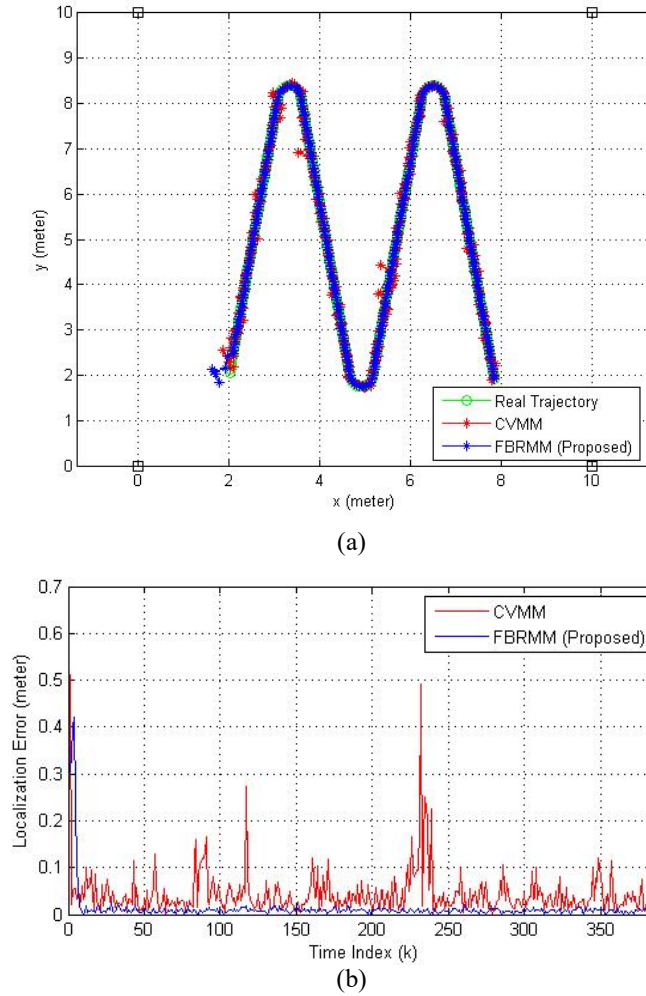


Fig. 4 MCL results when  $\mathbf{Q}_k = 50^2 \mathbf{I}_2$ : (a) real and estimated trajectory and (b) localization error.

#### 4. Conclusions

In this paper, we have proposed a new motion model called the FBRMM for the MCL in WSNs. The proposed FBRMM showed good performance regardless of the process noise, while the existing CVMM showed the performance depending on the selection of the process noise. By using the FBRMM, designers are free from the burden of process noise modeling. Moreover, the FBRMM relieves sample impoverishment in the MCL. Since the FBRMM has many advantages over the CVMM, it can be used for various localization systems. We plan to apply the FBRMM to the different filters, such as the EKF and the UKF.

#### 5. Acknowledgements

This work (Grants No. C0406948) was supported by Business for Cooperative R&D between industry, Academy, and Research Institute funded Korea Small and Medium business Administration in 2016.

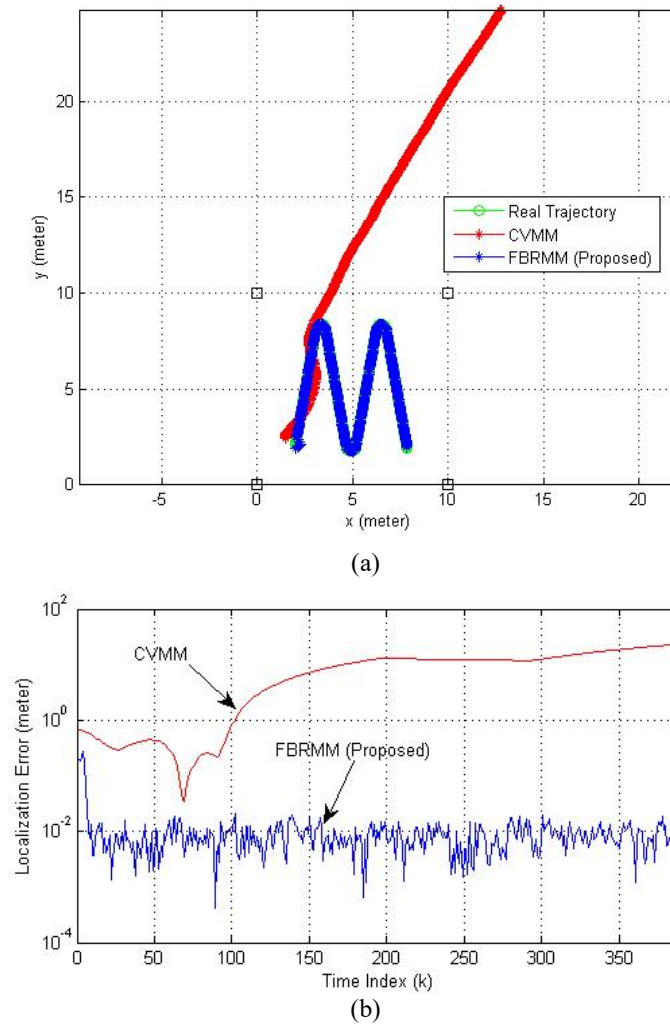


**Fig. 5** MCL results when  $\mathbf{Q}_k = 0.1^2 \mathbf{I}_2$ : (a) real and estimated trajectory and (b) localization error.

## 6. References

- [1] H. Liu, H. Darabi, P. Banerjee, and J. Liu, "Survey of wireless indoor positioning techniques and systems," *IEEE Trans. Systems, Man, and Cybernetics. Part C, Applications and Reviews*, Vol. 37, No. 6, pp. 1067–1080, Nov. 2007.
- [2] J. Pomarico-Franquiz and Y. S. Shmaliy, "Accurate self-localization in RFID tag information grids using FIR filtering," *IEEE Trans. Industrial Informatics.*, Vol. 10, No. 2, pp. 1317–1326, May 2014.
- [3] J. Pomarico-Franquiz, S. H. Khan, and Y. S. Shmaliy, "Combined extended FIR/Kalman filtering for indoor robot localization via triangulation," *Measurement*, Vol. 50, pp. 236–243, Apr. 2014.
- [4] J. M. Pak, C. K. Ahn, P. Shi, Y. S. Shmaliy, and M. T. Lim, "Distributed hybrid particle/FIR filtering for mitigating NLOS effects in TOA-based localization using wireless sensor networks," *IEEE Trans. Industrial Electronics*, to be published, doi: 10.1109/TIE.2016.2608897.
- [5] J. M. Pak, C. K. Ahn, Y. S. Shmaliy, P. Shi, and M. T. Lim, "Accurate and reliable human localization using composite particle/FIR filtering," *IEEE Trans. Human-Machine Systems*, to be published, doi: 10.1109/THMS.2016.2611826.

- [6] J. M. Pak, C. K. Ahn, Y. S. Shmaily, P. Shi, and M. T. Lim, "Switching extensible FIR filter bank for adaptive horizon state estimation with application," *IEEE Trans. Control Systems Technology*, Vol. 24, No. 3, pp. 1052–1058, May 2016.
- [7] J. M. Pak, C. K. Ahn, P. Shi, and M. T. Lim, "Self-recovering extended Kalman filtering algorithm based on model-based diagnosis and resetting using an assisting FIR filter," *Neurocomputing*, Vol. 173, Part 3, pp. 645–658, Jan. 2016.
- [8] J. M. Pak, C. K. Ahn, Y. S. Shmaily, and M. T. Lim, "Improving reliability of particle filter-based localization in wireless sensor networks via hybrid particle/FIR filtering," *IEEE Trans. Industrial Informatics*, Vol. 11, No. 5, pp. 1089–1098, Oct. 2015.
- [9] J. M. Pak, C. K. Ahn, M. T. Lim, and M. K. Song, "Horizon group shift FIR filter: An alternative nonlinear filter using finite recent measurements," *Measurement*, Vol. 57, pp. 33–45, Nov. 2014.
- [10] B. Ristic, S. Arulampalam, and N. Gordon, "Beyond the Kalman Filter: Particle Filters for Tracking Applications," *Artech House*, Norwood, MA, USA, 2004.
- [11] S. Thrun, W. Burgard, and D. Fox, "Probabilistic Robotics," *MIT Press*, Cambridge, MA, USA, 2005.
- [12] B. F. L. Scala and R. R. Bitmead, "Design of an extended Kalman filter frequency tracker," *IEEE Trans. Signal Processing*, Vol. 44, No. 3, pp. 739–742, Mar. 1996.
- [13] N. Oudjane and C. Musso, "Progressive correction for regularized particle filters," in *Proc. 3rd Int. Conf. Inf. Fusion, Paris, France, 2000*, pp. THB2/10–THB2/17.
- [14] B. Suh and T. J. Kim, "Operation of Sensor Nodes and Its Analysis for Wireless Sensor Networks with Mobility and Energy Harvesting," *Journal of KIIT*, Vol. 9, No. 1, pp. 119–125, Jan. 2011.
- [15] H. Kim, N. Kim, K. H. Kim, H. C. Bang, S. J. Kim, "Implementation of Robot Moving Mechanism for Localization in Wireless Sensor Networks," *Journal of KIIT*, Vol. 9, No. 3, pp. 147–153, March. 2011.
- [16] S.Y. Park, "Enhanced Two-Tier Clustering Scheme in Mobile Wireless Sensor Networks," *Journal of KIIT*, Vol. 12, No. 8, pp. 47–53, Aug. 2014.